BIOCHEMISTRY
including biophysical chemistry & molecular biology

Article

pubs.acs.org/biochemistry

Comparative Studies on the Late Bleaching Processes of Four Kinds of Cone Visual Pigments and Rod Visual Pigment

Keita Sato, Takahiro Yamashita, Yasushi Imamoto, and Yoshinori Shichida*

Department of Biophysics, Graduate School of Science, Kyoto University, Kyoto 606-8502, Japan

ABSTRACT: Visual pigments in rod and cone photoreceptor cells of vertebrate retinas are highly diversified photoreceptive proteins that consist of a protein moiety opsin and a light-absorbing chromophore 11-*cis*-retinal. There are four types of cone visual pigments and a single type of rod visual pigment. The reaction process of the rod visual pigment, rhodopsin, has been extensively investigated, whereas there have been few studies of cone visual pigments. Here we comprehensively investigated the reaction processes of cone visual pigments on a time scale of milliseconds to minutes, using flash photolysis equipment optimized for cone visual pigment photochemistry. We used chicken violet (L-group), chicken blue (M1-group), chicken green (M2-group), and monkey green (L-group) visual pigments as representatives of the respective groups of the phylogenetic tree of cone pigments. The S, M1, and M2 pigments showed the formation of a pH-dependent mixture of meta intermediates, similar to that formed from rhodopsin. Although monkey green (L-group) also formed a mixture of meta intermediates, pH dependency of meta intermediates was not observed. However, meta intermediates of monkey green became pH dependent when the chloride ion bound to the monkey green was replaced with a nitrate ion. These results strongly suggest that rhodopsin and S, M1, and M2 cone visual pigments share a molecular mechanism for activation, whereas the L-group pigment may have a special reaction mechanism involving the chloride-binding site.

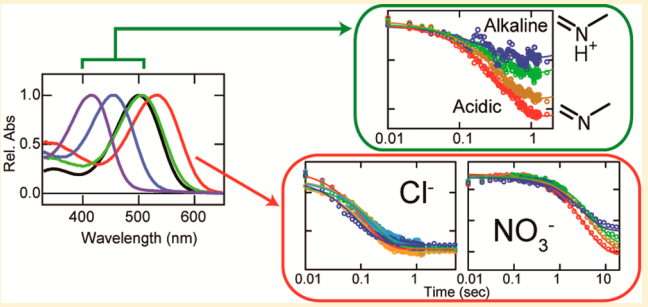

The visual transduction process in photoreceptor cells of vertebrate retinas begins with photon absorption by visual pigments. Visual pigments are retinal-based photoreceptive proteins belonging to the family of G protein-coupled receptors.[1] Phylogenetic analyses indicate that visual pigments are classified into four groups of cone visual pigments and a single rod visual pigment group. Rod and cone visual pigments possess molecular properties that correspond to their physiological role as scotopic and photopic light receptors.[1−3] The presence of multiple types of cone pigments with different absorption maxima is the molecular basis of color discrimination. To clarify the physiological roles of visual pigments, comparative analyses of molecular properties among cone visual pigments and that between rod and cone visual pigments are necessary.

Phylogenetic classification of cone visual pigments is well correlated to their absorption maxima, and they are referred to as S (SWS1), M1(SWS2), M2 (Rh2), and L (LWS)-groups.[4−7] The difference in absorption maximum among the three groups of cone visual pigments, except for the L-group cone visual pigments, is due to the differences in amino acid residues situated near the retinal chromophore. On the other hand, L-group cone visual pigments contain a chloride-binding site in their protein moieties and binding of chloride causes a red-shift of their absorption maxima. It has also been shown that nitrate can replace the chloride and bind to the chloride-binding site.[8] Moreover, UV−vis and FTIR spectroscopy studies have shown that the nitrate bound form is more similar to the anion unbound form than the chloride bound form.[9−11] Mutational analysis of human red and green pigments has identified the amino acid residues responsible for the chloride binding as histidine and lysine at position 181 and 184 (bovine rhodopsin numbering system), respectively.[12]

The photochemical and subsequent thermal reactions of rod visual pigment, rhodopsin, have been comprehensively studied, resulting in precise identification of the state that activates G protein. Namely, photon absorption causes *cis*−*trans* isomerization of the retinal chromophore, which induces conformational changes of the protein moiety, resulting in the formation of the G protein-activating state meta-II intermediate in equilibrium with its precursor, meta-I intermediate.[13] The equilibrium shifts in response to environmental pH, and the amounts of meta-I and -II intermediates increase in alkaline and acidic conditions, respectively.[14,15] Furthermore, recent studies have demonstrated that meta-II intermediate consists of two conformationally distinctive states: meta-IIa and meta-IIb intermediates.[16,17] Meta-I to meta-IIa conversion proceeds by intramolecular proton transfer from the retinal Schiff base to its counterion without proton exchange between the protein and its outer environment. The conversion from the meta-IIa to meta-IIb intermediate involves global conformational changes, but it is spectrally silent. Subsequently, the conformation of

Received: January 20, 2012
Revised: April 16, 2012
Published: May 9, 2012

   dx.doi.org/10.1021/bi3000885 | *Biochemistry* 2012, 51, 4300−4308

meta-IIb is stabilized by proton uptake from the outer environment to an amino acid residue (probably Glu134) in the cytoplasmic region of rhodopsin from the outer environment.[18,19] Therefore, the overall equilibrium among meta intermediates is pH-dependent.

The photochemical and subsequent thermal reactions of cone visual pigments have also been investigated, since the isolation a L-group cone visual pigment, iodopsin (chicken red-sensitive cone visual pigment), from chicken retinas.[20,21] Since then, several lines of evidence have shown that cone visual pigments also form a G protein-activating meta-II intermediate, through several thermolabile intermediates after the *cis*−*trans* isomerization of the retinal chromophore.[22−28] However, the thermal reactions of cone visual pigments are significantly faster than those of the rod visual pigment. Therefore, spectroscopic studies on the cone pigments, especially the formation of meta-II intermediate, have been greatly limited.

Here, we overcame the difficulty of studying cone visual pigments by improving the signal-to-noise ratio of the spectroscopic system used to measure their thermal reactions and succeeded in analyzing the formation and decay kinetics of the active states of cone visual pigments. The results clearly showed that four kinds of cone visual pigments exhibit similar but slightly different reaction processes. First, chicken violet exhibits a reaction process similar to that of rhodopsin, although the reactions proceed considerably faster than those of rhodopsin. That is, meta-I intermediate of chicken violet converts to a mixture of meta-I and meta-II intermediates, followed by formation of meta-III intermediate that decomposes into *all-trans*-retinal and opsin. Second, meta-I intermediates of chicken blue and chicken green convert to a mixture of three intermediates, meta-I, -II, and -III, instead of a mixture of two intermediates, meta-I and -II, and the mixture of three intermediates then decays into *all-trans*-retinal and opsin. These three cone visual pigments exhibit pH-dependent formation of the intermediates similar to that of rhodopsin. That is, meta-II favors acidic conditions. Third, the reaction of the L-group cone visual pigment monkey green was different from those of other cone pigments. Meta-I intermediate of monkey green also converts to a mixture of meta-I and meta-II intermediates. However, this process exhibited no pH dependence. Because L-group pigments have a chloride-binding site and chloride-binding effect (chloride effect) is diminished by replacement of chloride with nitrate, as described above, we tested the effect of anion replacement on kinetics and a pH dependence of meta intermediates. Interestingly, a pH-dependent shift of the relative amounts of meta-I and meta-II intermediates became detectable when a chloride ion was replaced with nitrate. On the basis of these results, similar and differing properties among rhodopsin and four kinds of the cone visual pigments examined are discussed.

MATERIALS AND METHODS

Sample Preparation. cDNAs encoding four kinds of cone visual pigments (chicken violet, chicken blue, chicken green, and monkey green (accession nos. M92039, M92037, M88178, and AF158975)[4,29,30] were tagged by the epitope sequence of the antibovine rhodopsin monoclonal antibody Rho1D4 (ETSQVAPA) at the C-terminus and were inserted into mammalian expression vector pCAG-GS. The cDNA of bovine rhodopsin was also inserted into mammalian expression vector pCAG-GS without tagging. The plasmid DNAs were transfected into HEK293T cells by the calcium phosphate methods. After incubation of the transfected cells for 2 days, they were collected by centrifugation and suspended in buffer A (140 mM NaCl, 3 mM $MgCl_2$, 50 mM HEPES, pH 7.0 at 20 °C), and 11-*cis*-retinal was added to the buffer (final retinal concentration 40 μM) to prepare the pigments. The following procedures were carried out on ice under dim red light unless otherwise noted. The pigments were extracted from the cells with buffer B (0.75% CHAPS, 1 mg/mL PC, 140 mM NaCl, 3 mM $MgCl_2$, 50 mM HEPES, pH 7.0 at 20 °C) and purified by chromatography on a column with the antibovine rhodopsin monoclonal antibody Rho1D4. The pH of the sample was adjusted by addition of NaOH or HCl. For samples at pH below 6.5, the sample was diluted with buffer containing 50 mM MES so that the buffer concentration was 25 mM HEPES and 25 mM MES, but other ingredients (detergent, PC, and salts) concentrations were the same as above.

To prepare nitrate bound form of monkey green, the extraction and purification procedures described above were performed using the buffers containing nitrate salts instead of chloride salts and HNO_3.

Spectrophotometry. Absorption spectra of the samples were recorded by a conventional spectrophotometer (Shimadzu UV2450). Time-resolved absorption spectra were recorded using two types of customized CCD spectrophotometers (Hamamatsu Photonics Co., Ltd.). One was able to continuously record the absorption spectra (360−616 nm) with a wavelength resolution of 1.57 nm at time intervals of 9.7 ms, and the other was able to record the spectra (250−900 nm) with a wavelength resolution of 0.353 nm at time intervals of 100 μs. The pigment solutions in buffer containing 0.75% CHAPS, 1 mg/mL PC, 140 mM NaCl, 3 mM $MgCl_2$, and 50 mM HEPES were used for samples at pH above 6.5, and those in buffer containing 0.75% CHAPS, 1 mg/mL PC, 140 mM NaCl, 3 mM $MgCl_2$, 25 mM HEPES, and 25 mM MES were used for samples at pH below 6.5. For measuring spectral changes of the nitrate bound form of monkey green, samples were prepared in buffer containing nitrate salts instead of chloride salts. The sample temperature was kept at 0 ± 0.1 °C by using a cell holder equipped with a Peltier device. The sample was irradiated with light passing through a glass cutoff filter (VL40, VY45, VY50, VY53; Toshiba Co., Ltd.) from a flash lamp (~10 μs; Nissin Electronic Co., Ltd.) 100 ms after the measurement began.

Data Analysis. The spectral changes of intermediates were analyzed by singular value decomposition (SVD) and global fitting methods as previously described, using the Igor Pro software program (WaveMetrics Inc.).[31,32] Briefly, the difference spectra were arranged in matrix A so that its columns and rows corresponded to wavelength and acquisition time. By SVD calculation, A was decomposed into a product of a left singular matrix U, a diagonal matrix containing singular values S, and a transpose of a right singular matrix V as follows:

$$A = U \times S \times V^{T} \quad (1)$$

The number of columns considered for the following estimation was determined based on the number of significant singular values and basis spectra in matrices U and V.

$$U \times S \times V^{T} \approx U_n \times S_n \times V_n^{T} \quad (2)$$

Assuming all the reactions were first-order reaction, V_n^{T} was fitted as follows by least-squares fitting:

$$V_n^{\mathrm{T}} = C \times (\exp(-t_i/\tau_1),\ \exp(-t_i/\tau_2),\ ...,\ \exp(-t_i/\tau_{n-1}),\ 1)^{\mathrm{T}} \quad (3)$$

The matrix C contained coefficient values of exponential function vectors $\exp(-t_i/\tau_j)$, where t_i represents acquisition time corresponding to that of the matrix A. On the basis of formulas 1, 2, and 3, the data matrix A can be expressed as follows:

$$A \approx U_n \times S_n \times C \times (\exp(-t_i/\tau_1),\ \exp(-t_i/\tau_2),\ ...,\ \exp(-t_i/\tau_{n-1}),\ 1)^{\mathrm{T}} \quad (4)$$

The jth column of the product of the matrices U_n , S_n, and C is the b-spectrum that denotes the spectral change in a single-exponential decay with time constant τ_j. The nth column of the matrix is the b_0-spectrum that shows the constant spectrum in bleached state. It should be noted that the opposite signed b-spectra are shown in Figures 2, 3, 5, and 6 for easy comparison.

RESULTS

Absorption Spectra of Rhodopsin and Four Kinds of Cone Visual Pigments. The phylogenetic tree of vertebrate visual pigments clearly shows that vertebrate visual pigments are classified into one group of rod visual pigment rhodopsin and four groups of cone visual pigments.[33,34] Thus, in the present study, we selected one rhodopsin (bovine rhodopsin) and four kinds of cone visual pigments (chicken violet, chicken blue, chicken green, and monkey green) that belong to the respective cone pigment groups. We have been trying to express chicken red (iodopsin) in cultured cells since identifying its sequence,[35] but it is still very difficult to express sufficient amounts of chicken red for spectroscopy. Therefore, we selected monkey green as a model of L-group cone visual pigments because the yield of monkey green was the best among the L-group cone visual pigments that we have tried to express (chicken red, monkey green, monkey red, human green, and human red).

Figure 1 shows the absorption spectra of these pigments that had been purified by immunoaffinity column chromatography after expression in HEK293 cells and solubilization with a CHAPS−PC mixture. The absorption maxima of bovine rhodopsin, chicken violet, chicken blue, chicken green, and monkey green were located at 500, 414, 454, 504, and 532 nm, respectively. The average optical purities of our samples of rhodopsin, chicken violet, chicken blue, chicken green, and monkey green were 2.0, 2.8, 2.5, 4.3, and 7.3, respectively.

Thermal Reactions of Rod and Cone Visual Pigments after Photon Absorption. The left panels of Figure 2 show the spectral changes measured in the time range of 10 ms to about 1000 s after pigments were photoexcited at 0 °C. The spectra shown in the right panels of Figure 2 are the b-spectra and the residuals calculated by global fitting procedures after singular value decomposition (SVD). The time constants of the respective b-spectra are shown in Table 1. The number of b-spectra represents the minimum number of reaction components involved in the spectral change. Our estimates show that photoirradiated rhodopsin comprises one reaction component in this time region, while cone visual pigments comprise two or three reactions components (Figure 2F−J). The reaction of photoirradiated rhodopsin is the conversion

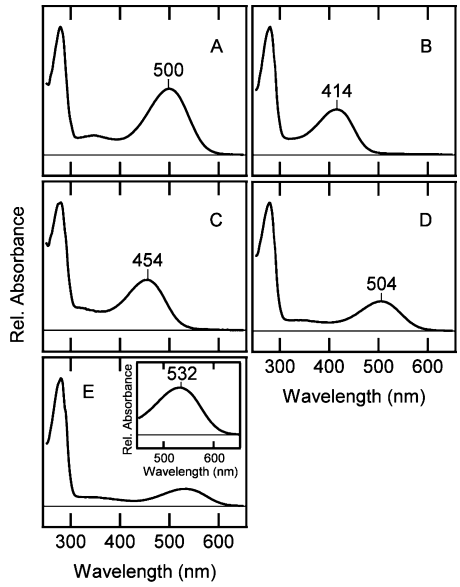

Figure 1. Absorption spectra of purified vertebrate visual pigments in the dark state. (A) Bovine rhodopsin, (B) chicken violet, (C) chicken blue, (D) chicken green, and (E) monkey green solubilized in buffer containing 0.75% CHAPS, 1 mg/mL PC, 140 mM NaCl, 3 mM $MgCl_2$, 50 mM HEPES. All spectra were recorded at 0 °C. The absorption maxima are indicated in the figures. Figure in (E) inset shows absorption spectrum of monkey green in the wavelength region from 450 to 650 nm.

from meta-I to meta-II. We examined the reaction processes of the respective cone visual pigments as follows.

We first examined the reaction process of chicken violet after irradiation with >380 nm light pulse (Figure 2B,G). The first process observed in the thermal reactions of photoirradiated chicken violet in this time range was the decrease of visible absorbance centered at about 450 nm with concurrent increase in UV absorbance centered at 380 nm. This reaction can be regarded as conversion of meta-I to meta-II of chicken violet, forming a mixture of meta-I and meta-II similar to rhodopsin reaction. The subsequent reaction was the conversion of this mixture to an intermediate having absorption maximum at about 420 nm, probably meta-III of chicken violet. Then, the third reaction was the decay of meta-III of chicken violet into retinal and opsin. The set of b-spectra obtained from the photoirradiated chicken violet at 0 °C are compared with those obtained from photoirradiated bovine rhodopsin at 20 °C in Figure 3 and reveal that these two pigments exhibited similar reactions, but the reactions of photoirradiated chicken violet occurred at lower temperature than those of photoirradiated bovine rhodopsin.[36]

Next, we examined the reaction processes of chicken blue and chicken green (Figure 2C,D,H,I). These two pigments exhibited two reaction components in the observed time range after irradiation with >430 or >480 nm light pulse. The first reactions were decreases of visible absorbance with concurrent increases in UV absorbance, which were very similar to those observed in rhodopsin and chicken violet. However, the second reactions were similar in profile to the third reaction observed in chicken violet. In other words, increases in visible absorbance were not observed in the reaction processes of chicken blue and green. These results suggest that formation of meta-III from a mixture of meta-I and meta-II does not occur in a separate manner in chicken blue or chicken green. Rather, in the

dx.doi.org/10.1021/bi3000885 | Biochemistry 2012, 51, 4300−4308

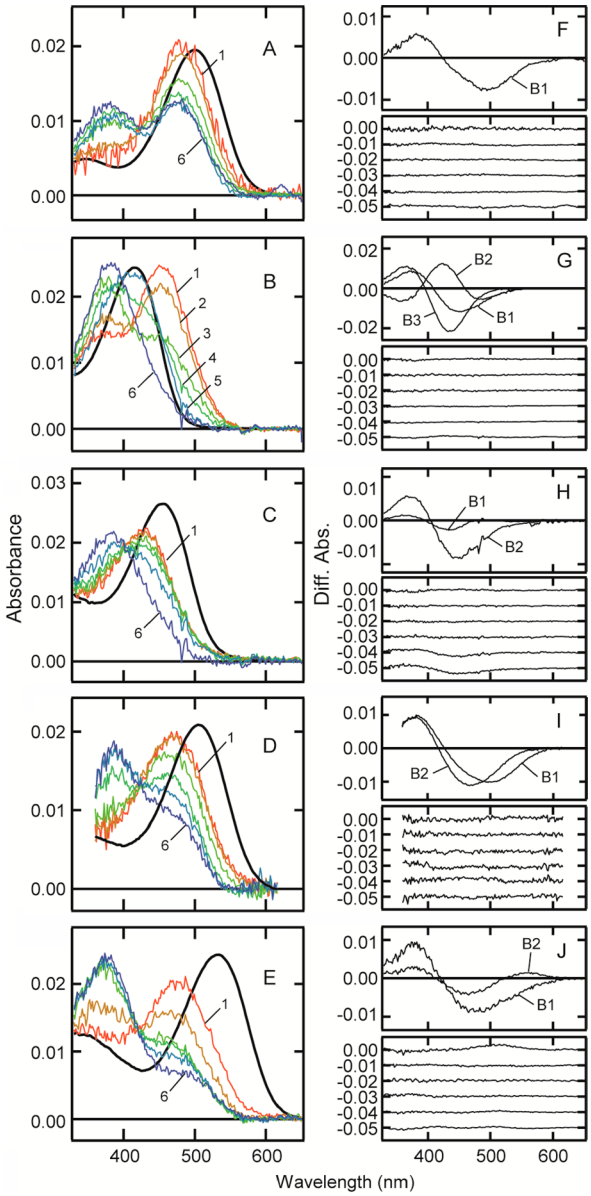

Figure 2. Overview of absorbance changes of vertebrate visual pigments after flash light irradiation. (A–E) The spectral changes of photointermediates were calculated by subtracting the spectra of unreacted residual pigments from the measured spectra at selected times after the sample irradiation. Solid black curves show the absorption spectra in the dark state. All the spectra were measured at 0 °C. (A) A set of absorption spectra of bovine rhodopsin at pH 7.1 measured 0.010, 0.10, 1.0, 11, 112, and 1107 s after irradiation (curves 1–6). (B) A set of absorption spectra of chicken violet at pH 7.1 measured 0.010, 0.10, 1.0, 11, 112, and 1107 s after irradiation (curves 1–6). (C) A set of absorption spectra of chicken blue at pH 7.0 measured 0.010, 0.10, 1.0, 11, 112, and 1107 s after irradiation (curves 1–6). (D) A set of absorption spectra of chicken green at pH 7.1 measured 0.0097, 0.097, 0.92, 13, 111, and 1184 s after irradiation (curves 1–6). (E) A set of absorption spectra of monkey green in the presence of chloride ion at pH 7.1 measured 0.010, 0.10, 1.0, 11, 112, and 1107 s after irradiation (curves 1–6). (F–J) Absorbance changes components were extracted by SVD and global fitting methods. Upper panels show the calculated set of b-spectra, and lower panels show the residuals calculated by simulating the experimental spectra with the set of b-spectra and the corresponding time constants. The data of bovine rhodopsin, chicken violet, chicken blue, chicken green, and monkey green are shown in (F), (G), (H), (I), and (J), respectively.

Table 1. Time Constants Corresponding b-Spectra at Neutral pH and pK_a in Equilibrium State

	time constants of b-spectra (s)			
sample	b1	b2	b3	pK_a
bovine rhodopsin	0.79			6.9
chicken violet	0.34	15	1195	7.4
chicken blue	0.86	266		7.0
chicken green	1.5	65		7.5
monkey green (Cl^-)	0.21	223		8.3
monkey green (NO_3^-)	4.5	490		7.5

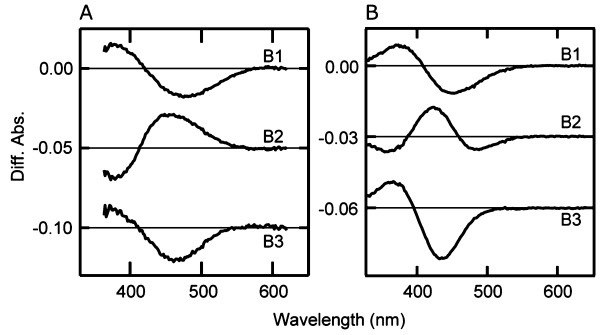

Figure 3. Similarity of the reaction processes of bovine rhodopsin and chicken violet. A set of b-spectra were calculated based on the time-resolved absorbance change data of (A) bovine rhodopsin at pH 5.9, 20 °C and (B) chicken violet at pH 7.1, 0 °C. The time constants were 0.067, 437, and 5131 s for the b1-, b2-, and b3-spectra of bovine rhodopsin and 0.34, 15, and 1195 s for the b1-, b2-, and b3-spectra of chicken violet, respectively.

reaction processes of chicken blue and chicken green, meta-I converts to a mixture of meta-I, meta-II, and meta-III, which then decays into retinal and opsin. According to the shape of the b2-spectra, meta-III of chicken blue has an absorption maximum at wavelength longer than that of meta-I of chicken blue, while meta-III of chicken violet and chicken green have absorption maxima at wavelengths shorter than those of their respective meta-I. The presence of a mixture of meta-I, meta-II, and meta-III in the reaction process is also suggested in the pH-dependent reaction of chicken blue and chicken green (see below).

The reactions observed for L-group cone visual pigment monkey green were different from those observed for rhodopsin, chicken violet, chicken blue, and chicken green (Figure 2E,J). The process in monkey green was composed of two reactions. The first was detected as a decrease of visible absorbance concurrent with an increase in UV absorbance and can be regarded as a conversion from meta-I to a mixture of meta-I and meta-II, which was similar to the first reaction of chicken violet. In the second reaction, the product having absorption maximum similar to that of meta-I converts to the UV-absorbing product and a product having absorption maximum longer than that of meta-I. It should be noted that low-temperature spectroscopy of chicken red (iodopsin) showed that most intermediates can convert back to the original pigment via thermal reactions.[32,37] Thus, it is likely that the product having absorption maximum longer than that of meta-I was the original monkey green that was formed from the thermal reaction of intermediates. It is difficult to determine from these data whether the product decaying in the second process included meta-III.

dx.doi.org/10.1021/bi3000885 | *Biochemistry* 2012, 51, 4300–4308

pH Dependence of the Spectral Changes of Rod and Cone Visual Pigments after Light Irradiation. It is well-known that the relative amounts of meta-I and meta-II in the mixture produced from rhodopsin are the functions of temperature and pH.[38] In fact, the time profile of the 480 nm absorbance in the range from 10 ms to about 1000 s after irradiation of rhodopsin depends on the sample pH (Figure 4A). In this range, the decrease of absorbance at 480 nm represents the conversion from meta-I to a mixture of meta-I and meta-II, and the subsequent unchanging region of absorbance represents the establishment of equilibrium between meta-I and meta-II. In Figure 4F, the absorbance at 480 nm in the range when equilibrium was established was plotted as a function of the sample pH. The apparent pK_a of the equilibrium was estimated to be about 7, which is in good agreement with that reported previously.[15,38]

The experimental data obtained for the four kinds of cone visual pigments were also analyzed in a similar way, and the results are shown in Figures 4B–E and 4G–J. The time constants of the reactions at several pHs are listed in Table 2. Chicken violet showed the formation of a mixture of meta-I and meta-II, the decay of this mixture to meta-III, and subsequent decomposition of meta-III into retinal and opsin in this time range. Chicken blue and chicken green showed the formation of a mixture of meta-I, meta-II, and meta-III and following decomposition into retinal and opsin. Interestingly, these cone visual pigments showed apparent pK_as of 7.4, 7.0, and 7.5, respectively, which are similar to that of rhodopsin (Table 1). This suggests that these cone visual pigments and rhodopsin utilize a similar molecular mechanism involving proton translocation.

Chicken violet exhibited a pH-dependent profile similar to those of chicken blue and chicken green. However, there was a clear difference between chicken violet and these other two pigments when the first b-spectra were compared. Figure 5A,B shows the b1-spectra calculated from the data obtained at pH 7.0, 7.5, and 8.0 of chicken violet and chicken green. For each pigment, the magnitudes of the b-spectra were different, but the b-spectra of chicken violet are superimposable when normalized at the maxima, while those of chicken green were not (Figure 4C,D). Superimposability of the b-spectra indicates that the reaction involves two components, and the relative amounts of these components depend on the pH of the sample. However, if the reaction involves three or more components, the shape of the b-spectrum depends on the pH of the sample. Therefore, the first reaction of chicken violet consists of the conversion from meta-I to meta-II, while that of chicken green consists of the conversion from meta-I to meta-II and -III.

The L-group pigment monkey green also showed a decrease of absorbance around 490 nm due to the decay of meta-I at an early stage and exhibited constant absorbance at a later stage (Figure 4E,J). However, the effect of pH on the time profile of the absorbance at 490 nm was much smaller than that for the other pigments. Thus, the equilibrium between meta-I and meta-II has little pH dependence, although the mixture of meta-I and meta-II is formed by irradiation of monkey green at various pHs.

Chloride Effects on L-Group Cone Visual Pigments. It is well-known that most L-group cone visual pigments have a chloride-binding site in their protein moieties, whereas other cone visual pigments do not.[12,39] Therefore, we examined whether or not chloride binding to L-group cone visual pigments is the cause of their difference in reaction process

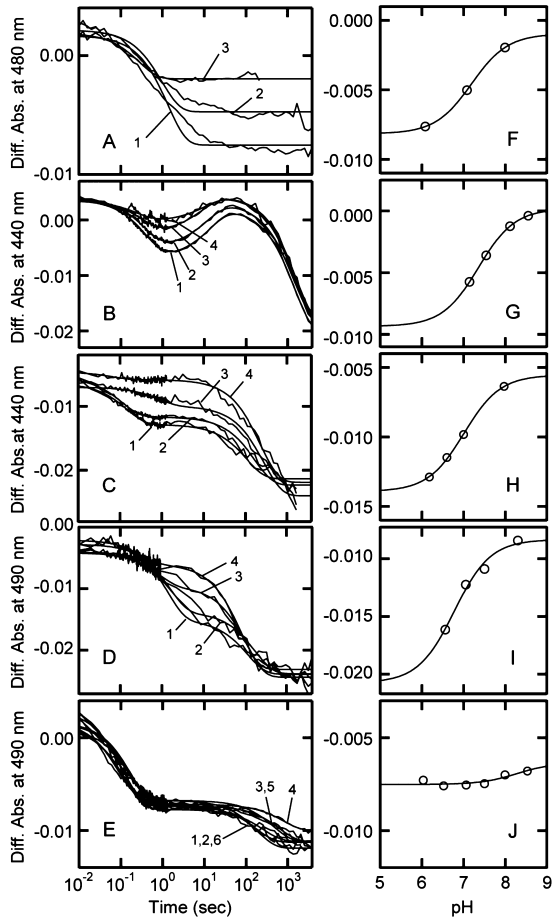

Figure 4. Kinetic profiles and the pH dependence of meta-intermediates. (A) The difference absorbances at 480 nm plotted against the incubation time after flash light irradiation of purified rhodopsin at pH 6.1, 7.1, and 8.0 (curves 1–3). They were simulated by single-exponential curves. (B) The difference absorbances at 440 nm plotted against the incubation time after flash light irradiation of purified chicken violet at pH 7.1, 7.5, 8.1, and 8.6 (curves 1–4). They were simulated by a combination of three sequential single-exponential curves. (C) The difference absorbances at 440 nm plotted against the incubation time after flash light irradiation of purified chicken blue at pH 6.2, 6.6, 7.0, and 8.0 (curves 1–4). They were simulated by a combination of two sequential single-exponential curves. (D) The difference absorbances at 490 nm plotted against the incubation time after flash light irradiation of purified chicken green at pH 6.6, 7.1, 7.5, and 8.3 (curves 1–4). They were simulated by a combination of two sequential single-exponential curves. (E) The difference absorbances at 490 nm plotted against the incubation time after flash light irradiation of purified monkey green with chloride ion at pH 6.0, 6.5, 7.1, 7.5, 8.0, and 8.5 (curves 1–6, respectively). They were simulated by a combination of two sequential single-exponential curves. (F–J) The difference absorbances at 60, 8.6, 1.7, 2.1, and 3.2 s in panels A–E plotted against the sample pH values, respectively. Solid lines are the best-fitted curves calculated based on the Henderson–Hasselbalch equation, and the pK_as were estimated from these curves.

from the other cone visual pigments. For this purpose, we prepared monkey green that had nitrate instead of chloride in the chloride-binding site and measured the reaction process after it was photoirradiated.

Figure 6 shows spectral changes observed for the nitrate-bound monkey green after photoirradiation (Figure 6A), b-spectra calculated by SVD analysis of the spectral changes followed by global fitting (Figure 6B), pH-dependent time

dx.doi.org/10.1021/bi3000885 | *Biochemistry* 2012, 51, 4300–4308

Table 2. Sample pHs and Corresponding Time Constants Estimated by Fitting the Data with Sum of Exponential Functions

sample	sample pH	time constants (s)		
bovine rhodopsin	6.1		1.3	
	7.1		0.97	
	8.0		0.28	
chicken violet	7.1	0.4	14	1459
	7.5	0.38	12	1387
	8.1	0.32	8.8	1542
	8.6	0.26	11	1559
chicken blue	6.2	0.15		107
	6.6	0.11		170
	7.0	0.88		282
	8.0	0.067		232
chicken green	6.6	1.1		125
	7.1	1.8		228
	7.5	1.4		142
	8.3	0.25		81
monkey green (Cl^-)	6.0	0.11		176
	6.5	0.13		107
	7.1	0.18		637
	7.5	0.17		809
	8.0	0.15		466
	8.5	0.88		184
monkey green (NO_3^-)	6.5	3.3		362
	7.1	4.7		411
	7.6	5.3		1116
	7.9	3.2		3288

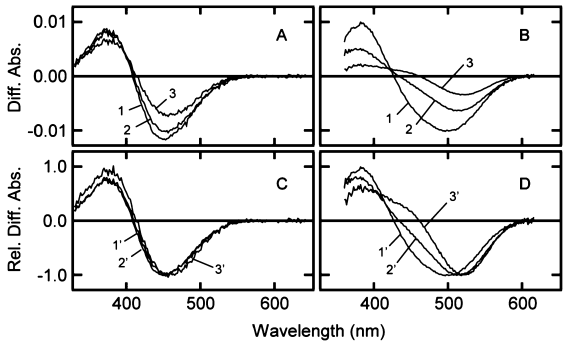

Figure 5. Qualitative difference between the first components of the absorbance changes of chicken green and violet. (A) A set of b1-spectra of chicken violet calculated based on the spectra measured for the sample at pH 7.1, 7.5, and 8.1 (curves 1–3). (B) A set of b1-spectra of chicken green calculated based on the spectra measured for the sample at pH 7.1, 7.5, and 8.3 (curves 1–3). (C, D) The b1-spectra normalized to the value at the negative peaks taken as −1.0. Curves 1′-3′ in panel C correspond to curves 1–3 in panel A, and the positions of the negative peaks are 452, 455, and 460 nm, respectively. Curves 1′-3′ in panel D correspond to curves 1–3 in panel B, and the positions of the negative peaks are 499, 513, and 521 nm, respectively.

profiles of absorbance at 470 nm (Figure 6C), and absorbance at 470 nm in the equilibrium state (Figure 6D). The nitrate-bound monkey green also underwent conversion of meta-I to a mixture of meta-I and meta-II and its decay into *all-trans*-retinal and opsin in addition to the conversion of the original pigment, which had absorption maximum at a longer wavelength than meta-I. From the pH-dependent changes of absorbance at 470 nm in the equilibrium state, the apparent pK_a was estimated to be 7.5. That is, by replacing chloride with nitrate, we also

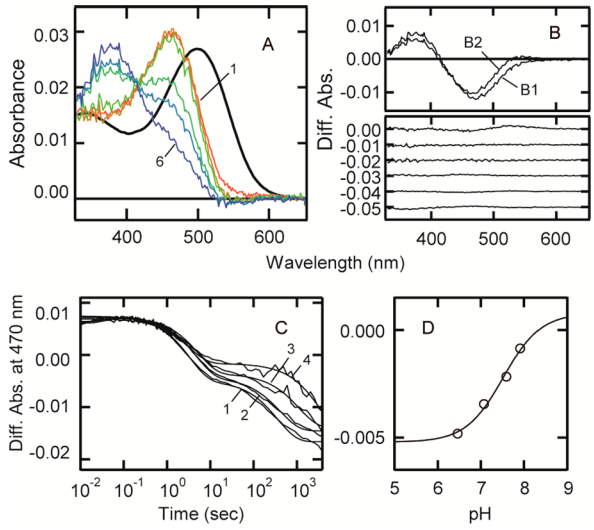

Figure 6. Effect of the replacement of the anion species by nitrate in the monkey green sample. (A) A set of absorption spectra of monkey green in the presence of nitrate ion at pH 7.1 measured at 0.010, 0.10, 1.0, 11, 112, and 1107 s after irradiation (curves 1–6). These spectra were calculated by subtracting the spectra of unreacted residual pigments from the measured spectra at selected times after the sample irradiation. The solid black curve shows the absorption spectrum in the dark state. The absorption maximum in the dark state is 498 nm. (B) The b-spectra and the residuals calculated based on the spectral data of monkey green with nitrate ion through SVD analysis and global fitting. (C) The difference absorbances at 470 nm plotted against the incubation time after flash light irradiation of purified monkey green with nitrate ion at pH 6.5, 7.1, 7.6, and 7.9 (curves 1–4). They were simulated by a combination of two sequential single-exponential curves. (D) The difference absorbances at 11 s in panel C plotted against the sample pH values. Solid line in the panel is the best-fitted curve calculated based on the Henderson–Hasselbalch equation. The pK_a was estimated to be 7.5.

observed a pH-dependent shift of the equilibrium for monkey green.

DISCUSSION

In the present study, we found that, like rhodopsin, cone visual pigments convert to a mixture of meta intermediates upon absorption of light, and the composition of the mixture is pH-dependent. Although L-group pigment monkey green exhibited no pH dependence, such dependence became detectable when chloride was replaced with nitrate. In addition, we found that the kinetics of the formation of meta-III are different among the pigments. The formation of meta-III of chicken violet occurs separately from the formation of meta-I and meta-II. This process is faster but otherwise similar to the formation of meta-III of rhodopsin. In contrast, meta-III of chicken blue and green is formed together with meta-II.

In addition to the absence of a pH-dependent equilibrium shift, the chloride-bound form of monkey green exhibits meta-I decay more than 10 times faster than that of its nitrate-bound form. It also forms the meta-I/meta-II mixture that contains a larger amount of meta-II than that of the nitrate-bound form. It would be easy to account for the absence of pH dependence, if the chloride-bound form of monkey green would not produce a meta-I/meta-II mixture but rather would undergo 100% conversion from meta-I to meta-II. However, the relative amounts of meta-I and -II of monkey green in the state at pH 7.1 were estimated to be 55 and 45%. Thus, the mechanism

dx.doi.org/10.1021/bi3000885 | *Biochemistry* 2012, 51, 4300–4308

accounting for the lack of pH dependence is not so simple. If proton uptake from the environment is essential for the formation of meta-II state in the chloride-bound form of monkey green like that in rhodopsin, amounts of the meta-I and meta-II in the mixture should be pH dependent, unless there is a "protonated meta-I state" in the mixture. Thus, one of the possibilities to account for the pH-independent formation of meta-I/meta-II mixture in the chloride-bound form of monkey green is the presence of the protonated meta-I state that has absorption characteristics similar to that of meta-I but has a proton acquired from the environment at the cytoplasmic region of the protein. The other possibility is that the proton is acquired from the environment upon binding of chloride in the chloride-binding site, and this proton transfers to the cytoplasmic region through hydrogen network system upon formation of meta-II state. That is, no proton uptake from the environment occurs in the conversion process of meta-I to meta-II in the chloride-bound form of monkey green. In any case, a more sophisticated experimental approach in combination with mutational analysis is required to solve this problem. In this context, it should be noted that more sophisticated analyses of the thermal reactions of rhodopsin intermediates have been already performed, resulting in identification of the substates of lumi, meta-I, and meta-II intermediates.[18,31,40] In contrast, experimental data obtained from cone visual pigments still have relatively large noises that hinder detailed analyses of the thermal reactions. Therefore, it will be our future research to search for the experimental conditions under which cone visual pigments are more stabilized and to optimize the spectroscopic measurements for cone visual pigments.

There are only a few reports about the pH dependence of photointermediates of cone pigments. Vissers and his colleagues showed that the meta-I/meta-II equilibrium observed for L-group pigment human green is different from that observed for rhodopsin; namely, the formation of meta-II was observed even in alkaline pH.[41] Our observations on the chloride-bound form of monkey green were consistent with that report. However, Liang and his colleagues showed that the meta-I/meta-II equilibrium of L-group pigment gecko P521 is altered by changing the pH of the sample, as observed for rhodopsin.[42] These differences in the pH-dependent profile could be resolved by the detailed experiments performed using uniform solution parameters, such as ionic strength, pH, and detergent, for the extraction of the pigment.

The physiological role of meta-III intermediate is still unknown even for rhodopsin. In previous reports, it was speculated that meta-III works as storage of *all-trans*-retinal to avoid the release of a large amount of *all-trans*-retinal to the cell environment in bright light conditions.[36,43] This hypothesis appears to be consistent with the kinetic properties of meta-III intermediate of rhodopsin, which is formed very slowly, and those of chicken violet, which is formed separately from meta-II. However, as shown in this study, meta-III of chicken blue and green is formed concurrently with meta-II. This difference in the kinetics of the formation and decay of meta-III should be considered in assessing the physiological role of meta-III.

For bovine rhodopsin, it has been shown that the primary proton acceptor from the outer environment is the glutamic acid in the E/DRY triad (Glu134), which is highly conserved in family 1 GPCRs.[19,44] The deprotonated carboxyl group of Glu134 forms a salt bridge with the guanidium group of Arg135, which in turn forms salt bridges with the carboxyl group of Glu247 and the hydroxyl group of Thr251.[45−47] These interactions form an ionic lock between helices III and VI and stabilize the inactive conformation in the dark state.[48,49] Upon formation of the active state, the ionic lock is broken, and protonation of Glu134 stabilizes the conformation of the active state. These four residues are well conserved in the rhodopsin group and the four cone pigment groups. Thus, the uptake by Glu134 of a proton from the solution environment could be a mechanism to stabilize the active state via the intramolecular proton translocation. In contrast, it has been shown that the active state of invertebrate rhodopsins such as squid rhodopsin is acid meta-rhodopsin, which has a protonated retinylidene Schiff base as its chromophore and forms under acidic conditions.[50] A vertebrate nonvisual pigment, parapinopsin, exhibits a pH-dependent shift in the equilibrium of the meta-intermediates quite similar to that of invertebrate rhodopsin, although it is phylogenetically close to vertebrate visual pigments.[51,52] In these pigments, the Schiff base of meta-intermediates is directly titrated by the solution environment of near-neutral pH. Therefore, the pH-dependent shift between meta-I and -II of vertebrate visual pigments is unique and was acquired after branching of the vertebrate visual pigments from parapinopsin in the course of molecular evolution. Thus, it is very likely that amino acid residues conserved in the vertebrate visual pigments but not in parapinopsins, such as Trp126 and Pro180, made some contribution to the acquisition of this mechanism. Future studies of the pH dependence of the meta-intermediates in other vertebrate nonvisual pigments such as pinopsin, VA opsin, and parietopsin will highlight the residues accounting for the different molecular bases of the active state formation between vertebrate and invertebrate rhodopsins.[53]

In summary, we have demonstrated that cone visual pigments, except for the L-group pigment, form a meta-II intermediates with similar mechanisms to that of rhodopsin. The L-group pigment also forms meta-II intermediate with a similar mechanism when chloride is replaced with nitrate. These results suggested that various visual pigments in vertebrates share a common molecular mechanism to activate the G protein, while the L-group cone visual pigment diversified.

AUTHOR INFORMATION

Corresponding Author

*Tel +81-75-753-4213; Fax +81-75-753-4210; e-mail shichida@rh.biophys.kyoto-u.ac.jp.

Funding

This work was supported by Grants-in-aid for Scientific Research and the Global Center of Excellence Program "Formation of a Strategic Base for Biodiversity and Evolutionary Research: from Genome to Ecosystem" from the Ministry of Education, Culture, Sports, Science and Technology, Japan to I.Y. and Y.S., by a JSPS Research Fellowship for Young Scientists to K.S. and by Takeda Science Foundation to T.Y.

Notes

The authors declare no competing financial interest.

ACKNOWLEDGMENTS

We thank Prof. R. S. Molday for the generous gift of a Rho1D4-producing hybridoma and Prof. H. Niwa for pCAG-GS vector. We are also grateful to Dr. E. Nakajima and Dr. T. Matsuyama for critical reading of our manuscript and invaluable comments.

■ ABBREVIATIONS

CHAPS, 3-[(3-cholamidopropyl)dimethylammonio]-propanesulfonate; PC, L-α-phosphatidylcholine.

■ REFERENCES

(1) Shichida, Y., and Imai, H. (1998) Visual pigment: G-protein-coupled receptor for light signals. *Cell. Mol. Life Sci. 54*, 1299−1315.

(2) Fu, Y., and Yau, K.-W. (2007) Phototransduction in mouse rods and cones. *Pflugers Arch. 454*, 805−819.

(3) Sakurai, K., Onishi, A., Imai, H., Chisaka, O., Ueda, Y., Usukura, J., Nakatani, K., and Shichida, Y. (2007) Physiological properties of rod photoreceptor cells in green-sensitive cone pigment knock-in mice. *J. Gen. Physiol. 130*, 21−40.

(4) Okano, T., Kojima, D., Fukada, Y., Shichida, Y., and Yoshizawa, T. (1992) Primary structures of chicken cone visual pigments: vertebrate rhodopsins have evolved out of cone visual pigments. *Proc. Natl. Acad. Sci. U. S. A. 89*, 5932−5936.

(5) Bowmaker, J. K. (2008) Evolution of vertebrate visual pigments. *Vision Res. 48*, 2022−2041.

(6) Yokoyama, S. (2008) Evolution of dim-light and color vision pigments. *Annu. Rev. Genomics Hum. Genet. 9*, 259−282.

(7) Shichida, Y., and Matsuyama, T. (2009) Evolution of opsins and phototransduction. *Philos. Trans. R. Soc., B 364*, 2881−2895.

(8) Tachibanaki, S., Imamoto, Y., Imai, H., and Shichida, Y. (1995) Effect of chloride on the thermal reverse reaction of intermediates of iodopsin. *Biochemistry 34*, 13170−13175.

(9) Hirano, T., Imai, H., Kandori, H., and Shichida, Y. (2001) Chloride effect on iodopsin studied by low-temperature visible and infrared spectroscopies. *Biochemistry 40*, 1385−1392.

(10) Hirano, T., Imai, H., and Shichida, Y. (2003) Effect of anion binding on the thermal reverse reaction of bathoiodopsin: anion stabilizes two forms of iodopsin. *Biochemistry 42*, 12700−12707.

(11) Hirano, T., Fujioka, N., Imai, H., Kandori, H., Wada, A., Ito, M., and Shichida, Y. (2006) Assignment of the vibrational modes of the chromophores of iodopsin and bathoiodopsin: low-temperature fourier transform infrared spectroscopy of ^{13}C- and ^{2}H-labeled iodopsins. *Biochemistry 45*, 1285−1294.

(12) Wang, Z., Asenjo, A. B., and Oprian, D. D. (1993) Identification of the chloride-binding site in the human red and green color vision pigments. *Biochemistry 32*, 2125−2130.

(13) Hofmann, K. P., Scheerer, P., Hildebrand, P. W., Choe, H.-W., Park, J. H., Heck, M., and Ernst, O. P. (2009) A G protein-coupled receptor at work: the rhodopsin model. *Trends Biochem. Sci. 34*, 540−552.

(14) Matthews, R. G., Hubbard, R., Brown, P. K., and Wald, G. (1963) Tautomeric forms of metarhodopsin. *J. Gen. Physiol. 47*, 215−240.

(15) Sato, K., Morizumi, T., Yamashita, T., and Shichida, Y. (2010) Direct observation of the pH-dependent equilibrium between metarhodopsins I and II and the pH-independent interaction of metarhodopsin II with transducin C-terminal peptide. *Biochemistry 49*, 736−741.

(16) Knierim, B., Hofmann, K. P., Ernst, O. P., and Hubbell, W. L. (2007) Sequence of late molecular events in the activation of rhodopsin. *Proc. Natl. Acad. Sci. U. S. A. 104*, 20290−20295.

(17) Mahalingam, M., Martínez-Mayorga, K., Brown, M. F., and Vogel, R. (2008) Two protonation switches control rhodopsin activation in membranes. *Proc. Natl. Acad. Sci. U. S. A. 105*, 17795−17800.

(18) Arnis, S., and Hofmann, K. P. (1993) Two different forms of metarhodopsin II: Schiff base deprotonation precedes proton uptake and signaling state. *Proc. Natl. Acad. Sci. U. S. A. 90*, 7849−7853.

(19) Arnis, S., Fahmy, K., Hofmann, K. P., and Sakmar, T. P. (1994) A conserved carboxylic acid group mediates light-dependent proton uptake and signaling by rhodopsin. *J. Biol. Chem. 269*, 23879−23881.

(20) Wald, G., Brown, P. K., and Smith, P. H. (1955) Iodopsin. *J. Gen. Physiol. 38*, 623−681.

(21) Yoshizawa, T., and Kuwata, O. (1991) Iodopsin, a red-sensitive cone visual pigment in the chicken retina. *Photochem. Photobiol. 54*, 1061−1070.

(22) Kandori, H., Mizukami, T., Okada, T., Imamoto, Y., Fukada, Y., Shichida, Y., and Yoshizawa, T. (1990) Bathoiodopsin, a primary intermediate of iodopsin at physiological temperature. *Proc. Natl. Acad. Sci. U. S. A. 87*, 8908−8912.

(23) Shichida, Y., Okada, T., Kandori, H., Fukada, Y., and Yoshizawa, T. (1993) Nanosecond laser photolysis of iodopsin, a chicken red-sensitive cone visual pigment. *Biochemistry 32*, 10832−10838.

(24) Shichida, Y., Imai, H., Imamoto, Y., Fukada, Y., and Yoshizawa, T. (1994) Is chicken green-sensitive cone visual pigment a rhodopsin-like pigment? A comparative study of the molecular properties between chicken green and rhodopsin. *Biochemistry 33*, 9040−9044.

(25) Kojima, D., Imai, H., Okano, T., Fukada, Y., Crescitelli, F., Yoshizawa, T., and Shichida, Y. (1995) Purification and low temperature spectroscopy of gecko visual pigments green and blue. *Biochemistry 34*, 1096−1106.

(26) Imai, H., Imamoto, Y., Yoshizawa, T., and Shichida, Y. (1995) Difference in molecular properties between chicken green and rhodopsin as related to the functional difference between cone and rod photoreceptor cells. *Biochemistry 34*, 10525−10531.

(27) Imai, H., Terakita, A., Tachibanaki, S., Imamoto, Y., Yoshizawa, T., and Shichida, Y. (1997) Photochemical and biochemical properties of chicken blue-sensitive cone visual pigment. *Biochemistry 36*, 12773−12779.

(28) Imai, H., Kuwayama, S., Onishi, A., Morizumi, T., Chisaka, O., and Shichida, Y. (2005) Molecular properties of rod and cone visual pigments from purified chicken cone pigments to mouse rhodopsin in situ. *Photochem. Photobiol. Sci. 4*, 667−674.

(29) Wang, S. Z., Adler, R., and Nathans, J. (1992) A visual pigment from chicken that resembles rhodopsin: amino acid sequence, gene structure, and functional expression. *Biochemistry 31*, 3309−3315.

(30) Onishi, A., Koike, S., Ida-Hosonuma, M., Imai, H., Shichida, Y., Takenaka, O., Hanazawa, A., Komatsu, H., Mikami, A., Goto, S., Suryobroto, B., Farajallah, A., Varavudhi, P., Eakavhibata, C., Kitahara, K., and Yamamori, T. (2002) Variations in long- and middle-wavelength-sensitive opsin gene loci in crab-eating monkeys. *Vision Res. 42*, 281−292.

(31) Tachibanaki, S., Imai, H., Mizukami, T., Okada, T., Imamoto, Y., Matsuda, T., Fukada, Y., Terakita, A., and Shichida, Y. (1997) Presence of two rhodopsin intermediates responsible for transducin activation. *Biochemistry 36*, 14173−14180.

(32) Imamoto, Y., and Shichida, Y. (2008) Thermal recovery of iodopsin from photobleaching intermediates. *Photochem. Photobiol. 84*, 941−948.

(33) Yoshizawa, T. (1994) Molecular basis for color vision. *Biophys. Chem. 50*, 17−24.

(34) Yokoyama, S. (2000) Molecular evolution of vertebrate visual pigments. *Prog. Retinal Eye Res. 19*, 385−419.

(35) Kuwata, O., Imamoto, Y., Okano, T., Kokame, K., Kojima, D., Matsumoto, H., Morodome, A., Fukada, Y., Shichida, Y., and Yasuda, K. (1990) The primary structure of iodopsin, a chicken red-sensitive cone pigment. *FEBS Lett. 272*, 128−132.

(36) Bartl, F. J., and Vogel, R. (2007) Structural and functional properties of metarhodopsin III: recent spectroscopic studies on deactivation pathways of rhodopsin. *Phys. Chem. Chem. Phys. 9*, 1648−1658.

(37) Imamoto, Y., Imai, H., Yoshizawa, T., and Shichida, Y. (1994) Thermal recovery of iodopsin from its meta I-intermediate. *FEBS Lett. 354*, 165−168.

(38) Parkes, J. H., and Liebman, P. A. (1984) Temperature and pH dependence of the metarhodopsin I-metarhodopsin II kinetics and equilibria in bovine rod disk membrane suspensions. *Biochemistry 23*, 5054−5061.

(39) Fager, L. Y., and Fager, R. S. (1979) Halide control of color of the chicken cone pigment iodopsin. *Exp. Eye Res. 29*, 401−408.

(40) Szundi, I., Lewis, J. W., and Kliger, D. S. (2003) Two intermediates appear on the lumirhodopsin time scale after rhodopsin photoexcitation. *Biochemistry 42*, 5091−5098.
(41) Vissers, P. M., Bovee-Geurts, P. H., Portier, M. D., Klaassen, C. H., and Degrip, W. J. (1998) Large-scale production and purification of the human green cone pigment: characterization of late photo-intermediates. *Biochem. J. 330* (Pt 3), 1201−1208.
(42) Liang, J., Govindjee, R., and Ebrey, T. G. (1993) Metarhodopsin intermediates of the gecko cone pigment P521. *Biochemistry 32*, 14187−14193.
(43) Heck, M., Schädel, S. A., Maretzki, D., Bartl, F. J., Ritter, E., Palczewski, K., and Hofmann, K. P. (2003) Signaling states of rhodopsin. Formation of the storage form, metarhodopsin III, from active metarhodopsin II. *J. Biol. Chem. 278*, 3162−3169.
(44) Fahmy, K., Sakmar, T. P., and Siebert, F. (2000) Transducin-dependent protonation of glutamic acid 134 in rhodopsin. *Biochemistry 39*, 10607−12.
(45) Li, J., Edwards, P. C., Burghammer, M., Villa, C., and Schertler, G. F. X. (2004) Structure of bovine rhodopsin in a trigonal crystal form. *J. Mol. Biol. 343*, 1409−1438.
(46) Okada, T., Sugihara, M., Bondar, A.-N., Elstner, M., Entel, P., and Buss, V. (2004) The retinal conformation and its environment in rhodopsin in light of a new 2.2 A crystal structure. *J. Mol. Biol. 342*, 571−583.
(47) Vogel, R., Mahalingam, M., Lüdeke, S., Huber, T., Siebert, F., and Sakmar, T. P. (2008) Functional role of the "ionic lock"--an interhelical hydrogen-bond network in family A heptahelical receptors. *J. Mol. Biol. 380*, 648−655.
(48) Acharya, S., and Karnik, S. S. (1996) Modulation of GDP release from transducin by the conserved Glu134-Arg135 sequence in rhodopsin. *J. Biol. Chem. 271*, 25406−25411.
(49) Ramon, E., Cordomí, A., Bosch, L., Zernii, E. Y., Senin, I. I., Manyosa, J., Philippov, P. P., Pérez, J. J., and Garriga, P. (2007) Critical role of electrostatic interactions of amino acids at the cytoplasmic region of helices 3 and 6 in rhodopsin conformational properties and activation. *J. Biol. Chem. 282*, 14272−14282.
(50) Hubbard, R., and George, R. C., St. (1958) The rhodopsin system of the squid. *J. Gen. Physiol. 41*, 501−528.
(51) Koyanagi, M., Kawano, E., Kinugawa, Y., Oishi, T., Shichida, Y., Tamotsu, S., and Terakita, A. (2004) Bistable UV pigment in the lamprey pineal. *Proc. Natl. Acad. Sci. U. S. A. 101*, 6687−6691.
(52) Terakita, A., Koyanagi, M., Tsukamoto, H., Yamashita, T., Miyata, T., and Shichida, Y. (2004) Counterion displacement in the molecular evolution of the rhodopsin family. *Nat. Struct. Mol. Biol. 11*, 284−289.
(53) Sato, K., Yamashita, T., Ohuchi, H., and Shichida, Y. (2011) Vertebrate Ancient-Long Opsin Has Molecular Properties Intermediate between Those of Vertebrate and Invertebrate Visual Pigments. *Biochemistry 50*, 10484−10490.